Research Article BEU Fen Bilimleri Dergisi 15(2): 583-593 (2026) DOI: 10.17798/bitlisfen.1799077

BİTLİS EREN UNIVERSITY
FEN BİLİMLERİ DERGİSİ
ISSN: 2147-3129 / e-ISSN: 2147-3188

SINGLE-STEP FABRICATION OF CHITOSAN-CONTAINING 3D NANOFIBER SCAFFOLD FOR BONE TISSUE ENGINEERING

Ozay EROGLU [1], H. Sevval DERE [1], Ugur ERKARSLAN [2], **Hulya SUBASAT [1]***

[1] *Muğla Sıtkı Koçman University, Department of Energy, Molecular Nano-Materials Laboratory, Muğla, Türkiye*
[2] *Muğla Sıtkı Koçman University, Department of Physics, Molecular Nano-Materials Laboratory, Muğla, Türkiye*
*** Corresponding Author:** hsubasat@mu.edu.tr

Article Info

Received: *October 7, 2025*
Revised: *November 24, 2025*
Accepted: *December 23, 2025*

Keywords
Bone Tissue Engineering,
Nanofiber Scaffolds,
Chitosan,
Electrospinning,
Hydroxyapatite.

ABSTRACT

Rising life expectancy and the growing incidence of trauma- and degeneration-related bone defects have increased demand for bone grafting and regeneration procedures, highlighting the need for effective alternatives to autografts and allografts. Bone tissue engineering addresses this need by providing biomimetic scaffolds that encourage cell infiltration and vascularization while matching key properties of native tissue. Here, we report the development of compressible, easily shapeable three-dimensional (3D) composite fibrous scaffolds intended to fill bone defects with irregular geometries. Scaffolds were fabricated in a single step by electrospinning polycaprolactone (PCL; FDA-approved polyester) blended with gelatin (GEL), chitosan (CS), and varying amounts of nano-hydroxyapatite (nHA). A specially designed spherical collector enabled formation of a cotton-like 3D architecture with high porosity and an interconnected fiber network. Scanning electron microscopy confirmed successful generation of the 3D nanofiber structure and enhanced pore interconnectivity. The resulting scaffolds exhibited a moldable, spring-like behavior, allowing packing into complex defect sites without losing structural integrity. Functional performance was evaluated via water vapor transmission rate, swelling, and in vitro biodegradation assays. The composites demonstrated appropriate moisture permeability, high water uptake, and a controlled degradation profile, suggesting a favorable microenvironment for tissue regeneration. Overall, the 3D PCL/GEL/CS/nHA cotton-like scaffolds combine mechanical conformability with porous nanofibrous morphology and tunable bioactivity, indicating strong potential as a defect-filling platform for bone tissue engineering applications. Composition was optimized to maximize 3D expansion, fiber uniformity, and nHA dispersion, providing osteoconductive cues. The platform is therefore suitable for subsequent cell-based validation and preclinical evaluation in irregular defect models.

1. INTRODUCTION

Bone possesses a unique ability to regenerate in response to injuries during skeletal development or adulthood, making bone repair a regenerative process distinct from the scar tissue formation typical of soft tissues [1]. Fracture healing is among the most common forms of bone regeneration observed in clinical settings [2]. However, certain conditions, such as severe injuries, infections, or diseases like osteoporosis, can impair this process, often necessitating bone grafting [3]. Bone grafting techniques include autografts, allografts, and synthetic substitutes. Autografts, considered the gold standard, utilize the patient's own bone, eliminating tissue compatibility issues. Allografts, sourced from donors or cadavers, are a viable alternative but present risks such as disease transmission and compromised mechanical properties. To address these limitations, research has increasingly focused on developing synthetic bone substitutes [4]. Globally, bone grafting is the second most common tissue transplantation procedure after blood transfusions [5]. Annually, over 2.2 million grafting procedures are performed for conditions like non-union fractures, spinal fusion, and joint arthrodesis, with an estimated cost exceeding $10 billion [6]. The projected doubling of osteoporotic fracture risks by 2040 underscores the

License: CC BY-NC 4.0

need for innovative synthetic grafts that combine scaffolds with biological elements to stimulate cell infiltration and bone formation [7].

Tissue engineering offers a promising approach to bone regeneration, focusing on repairing tissues using cells, growth factors, and scaffolds made from biodegradable and biocompatible materials [8]. Three-dimensional (3D) scaffolds play a critical role in facilitating cell transport, proliferation, and differentiation while mimicking the extracellular matrix (ECM). Biodegradable and biocompatible scaffolds are essential for supporting bone regeneration, providing a temporary platform that degrades as new bone forms [9], [10]. Electrospinning has emerged as a preferred technique for fabricating nanofiber-based scaffolds due to its simplicity, cost-effectiveness, and ability to create highly porous structures resembling the bone ECM [11]. However, a single polymer cannot meet all the mechanical, hydrophilic, and degradation requirements of an ideal scaffold. Thus, combining materials to form composites can enhance scaffold performance. Gelatin (GEL), derived from collagen degradation, supports cell adhesion and proliferation but lacks sufficient mechanical strength and stability for standalone use [12]. Polycaprolactone (PCL), known for its durability and slower degradation, complements GEL effectively. The PCL/GEL combination has been shown to improve biomechanical properties and cellular compatibility [13].

Incorporating chitosan (CS) into PCL/GEL/CS/nHA composite material enhances its suitability for bone tissue engineering by providing several key benefits. Chitosan is a natural polymer renowned for its biocompatibility and biodegradability, which are essential for biomedical applications [14]. Its degradation products are non-toxic and can be easily absorbed or excreted by the body, minimizing the risk of adverse reactions. Additionally, chitosan exhibits inherent antimicrobial properties, aiding in the prevention of infections at the implantation site—a critical factor in bone tissue engineering where infections can significantly impede healing. The cationic nature of chitosan facilitates interactions with negatively charged cell membranes, thereby promoting cell adhesion and proliferation. This characteristic supports the integration of the scaffold with surrounding tissues and encourages new bone formation. Moreover, chitosan-based scaffolds are osteoconductive, meaning they support the attachment and growth of osteoblasts, the cells responsible for bone formation, which is vital for successful bone regeneration. However, pure chitosan scaffolds often lack the mechanical strength required for load-bearing applications. To address this limitation, chitosan is frequently combined with other materials, such as polycaprolactone (PCL) and nano-hydroxyapatite (nHA), to enhance its mechanical properties while retaining its biological advantages [15], [16].

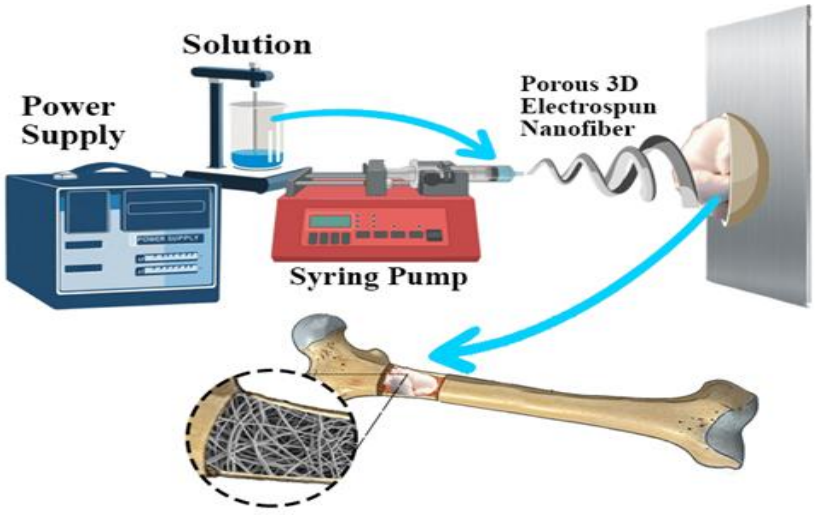


Figure 1. Schematic representation of the electrospinning process for fabricating 3D PCL/GEL/CS/nHA nanofiber scaffolds.

This research builds upon prior investigations by creating innovative 3D scaffolds with cotton-like characteristics and high moldability. These scaffolds were produced using an adaptable electrospinning method and a specially designed spherical collector, as shown in Figure 1. The structural components

were made from PCL, GEL, and CS polymers, which have previously shown promise in bone tissue engineering due to their biocompatibility and ability to support tissue growth. These advanced composite scaffolds mimic the bone's extracellular matrix (ECM) properties and overcome limitations associated with traditional 2D materials in bone regeneration and treating persistent bone fractures.

2. MATERIAL and METHOD

Commercial sources supplied the materials for this study, with analytical-grade chemical solvents used as received. Poly(ε-caprolactone) (PCL) with an approximate molecular weight of 80,000, bovine skin-derived gelatin (GEL) (Type B), Chitosan (CS, medium molecular weight), trifluoroethanol (TFE) and phosphate buffer saline (PBS) were acquired from Sigma-Aldrich (St. Louis, MO, USA). Nanohydroxyapatite with a particle size of 200 nm was obtained commercially from Nanografi (Ankara, Türkiye)

2.1. Preparation of PCL/GEL/CS/nHA Solution

The preparation of the PCL/GEL/CS solution followed the protocol outlined by Gautam et al. (2014). Separate solutions of 10% (w/v) PCL and 12% (w/v) GEL were created in TFE at ambient temperature. These solutions were then mixed in equal parts (PCL:GEL 50:50) and agitated for 24 hours at room temperature to ensure uniformity. Next, 2.2% (w/v) CS was added to this mixture and stirred for 24 h at room temperature, resulting in a homogeneous PCL/GEL/CS (w/w) 40:40:20 ratio solution. In the final step, nHA was introduced to this solution in various proportions (5-15%). The resulting mixtures were first homogenized using a magnetic stirrer, followed by an ultrasonic bath treatment.

2.2. Production of 3D Nanofibers by Electrospinning

The production of nanofibers was accomplished using the Spingenix SG100 electrospinning system (Figure 2). Prepared polymer solutions were loaded into 5 cc syringes fitted with 22-gauge blunt needles and placed in the syringe pump connected to the electrospinning machine. The electrospinning procedure involved depositing the solutions onto a specially designed spherical collector, with an applied voltage ranging from 15 to 20 kV and a flow rate between 0.4 and 1.2 mL/h.

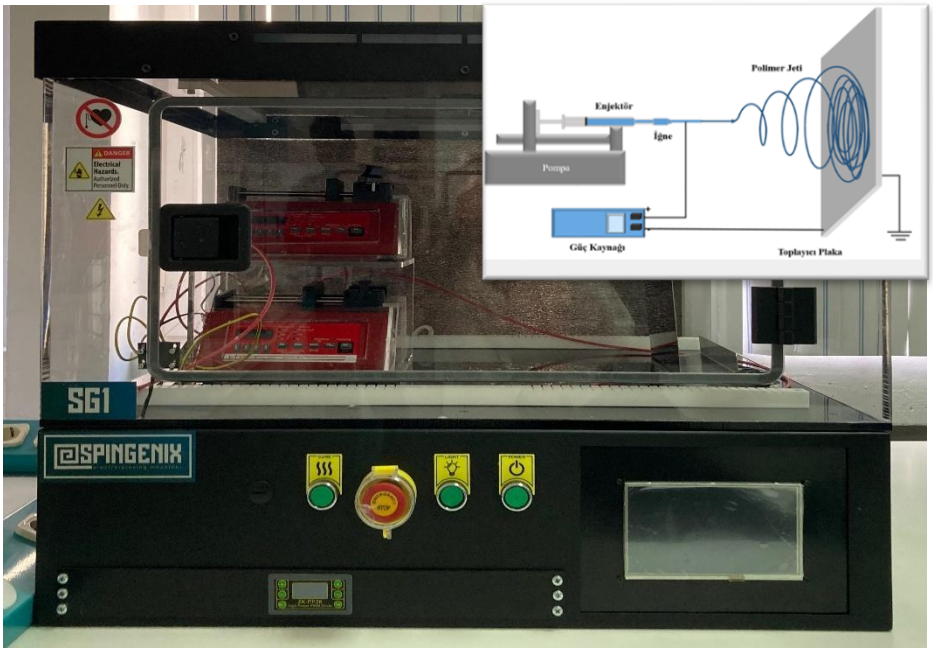


Figure 2. Illustration of the Electrospinning Device.

2.3. Morphological Study

The surface morphology and fiber architecture of the electrospun scaffolds were examined using ZEISS GEMINI-500 FESEM. Prior to imaging, samples were sputter-coated with a thin layer of gold to enhance electrical conductivity. SEM micrographs were obtained at various magnifications to evaluate

fiber uniformity, porosity, and structural integrity. Fiber diameter distributions were determined by analyzing at least 100 fibers per sample using ImageJ software (NIH, USA). The average fiber diameter and standard deviation were calculated and reported. Morphological differences between scaffolds with and without HA incorporation were comparatively assessed to observe potential changes in fiber continuity and porosity.

2.4. FTIR Spectroscopy

Fourier-transform infrared (FTIR) spectroscopy was employed to identify the chemical structure and verify the presence of specific functional groups in the fabricated scaffolds. Spectra were recorded using the Perkin Elmer, Spectrum 65 device over a wavenumber range of 4000–500 cm^{-1}.

2.5. WVTR Test

The water vapor transmission rate (WVTR) test was conducted using the container method. For this purpose, glass containers were filled with approximately 10 mL of distilled water, and their initial weights (W_0) were recorded. Nanofiber scaffold was then placed over the openings of the containers and securely sealed. The sealed containers were incubated in an oven at 37 ± 0.5°C for 24 hours. Following the incubation period, the nanofiber scaffolds were removed, and the final weights of the containers (W_t) were measured. The measurements were performed in triplicate. Based on these measurements, the water vapor permeability rate of the scaffold (mg/m^2h) was calculated using the equation 1 [17].

$$WVTR = \frac{W_0 - W_t}{Axt} \tag{1}$$

2.6. Swelling Test

Swelling test was assessed to determine the hydrophilicity and water absorption capacity of the scaffolds. For the tests, each sample was cut into 15 cm^2 sections in duplicate sets. Initially, the dry weights (W_0) of the scaffolds were recorded. The samples were then immersed in 10 mL of phosphate-buffered saline (PBS; pH 7.4) and incubated at 37 ± 0.5°C. On days 3, 7 and 14 of incubation, the scaffolds were carefully removed from the solution, blotted to remove excess surface liquid, and weighed (W_t). All measurements were conducted in triplicate. The swelling ratio (%) was calculated using Equation 2 [18]:

$$Swelling\ Ratio\ (\%) = \frac{W_t - W_0}{W_0} \tag{2}$$

2.7. Biodegradation Study

The biodegradation behavior of the scaffolds was investigated by monitoring their mass loss over time under physiological conditions. For this purpose, the scaffolds were cut into 15 cm^2 sections, and their initial dry weights (W_0) were recorded. The samples were then incubated in phosphate-buffered saline (PBS; pH 7.4) at 37°C. At predetermined time intervals (days 3, 7 and 14), the samples were removed from the solution, dried, and weighed to obtain the residual weights (W_t). All measurements were performed in triplicate. The degradation rate was calculated as the percentage of weight loss using Equation 3 [19]:

$$Degradation\ Rate\ (\%) = \frac{W_t - W_0}{W_0} x100 \tag{3}$$

3. RESULTS and DISCUSSION

3.1. Electrospinning Process and Optimizing Parameters

Ideal nanofibers should display a consistent distribution, smooth surface, and lack bead formations. Based on the porosity of nanofibers created from various proportions of PCL, GEL, CS, and nHA solution blends, the mixture ratios showing considerable promise for bone tissue engineering

applications were chosen for experimentation. In cases where nanofibers with suitable morphology were not achieved, the concentrations and mixture ratios were modified, and the system was fine-tuned following the approach outlined in the literature [20]. Critical factors such as voltage, flow rate, and distance between needle and collector were methodically optimized to produce flawless nanofibers with the desired morphological traits. The optimization process aimed to ensure uniform fiber formation, reduce bead structures, and generate a cotton-like, low-density structure appropriate for 3D scaffolds. The nanofibers gathered on the spherical collector demonstrated a three-dimensional, low-density, uncompressed structure similar to a cotton ball. The PCL/GEL solution formulated at a 40:40:20 (PCL/GEL/CS) ratio was enhanced with 5%, 10%, and 15% nHA, respectively, and the system was optimized using the electrospinning parameters listed in Table 1.

Table 1. Optimization of electrospinning parameters for nanofiber fabrication

PCL/GEL/CS Ratio (v/v)	HA Concentration (%)	Distance (cm)	Voltage (kV)	Flow Rate (mL/min)
40 / 40 / 20	5%	21	20	0.08
40 / 40 / 20	10%	17	22	0.10
40 / 40 / 20	15%	19	22	0.13

3.2. Morphology

Scanning electron microscopy (SEM) analysis of PCL/GEL/CS/nHA (5%, 10%, 15%) nanofiber scaffolds produced through electrospinning is depicted in Figure 3. The SEM images reveal that the nanofibers form a random, three-dimensional arrangement, creating an ideal environment for cellular activities such as adhesion, proliferation, and differentiation. SEM image analysis determined the porosity of scaffolds with 5%, 10%, and 15% nHA to be 79%, 76%, and 70%, respectively. The average diameters of the nanofibers were measured at 950 ± 44 nm, 850 ± 45 nm, and 775 ± 11 nm. Typically, smaller fiber diameters lead to decreased pore sizes in nanofiber scaffolds [21]. Higher concentrations of nHA result in thinner fiber diameters, allowing cells to make more extensive contact with the scaffold surface. Previous studies have shown that this enhanced contact promotes cellular behaviors like adhesion and growth [22]. The combination of the three-dimensional nanofiber structure and the osteoinductive properties of nHA creates an optimal environment for cell migration and growth, particularly beneficial for bone regeneration.

The three-dimensional, compressible, and moldable attributes of the scaffolds are depicted in Figure 4. These scaffolds demonstrate compressibility (a, c, d) and malleability (e, f, g), showcasing their versatility for clinical use. This unique characteristic highlights the scaffolds' ability to adjust to irregularly shaped bone defects, thereby increasing their effectiveness in bone tissue engineering applications.

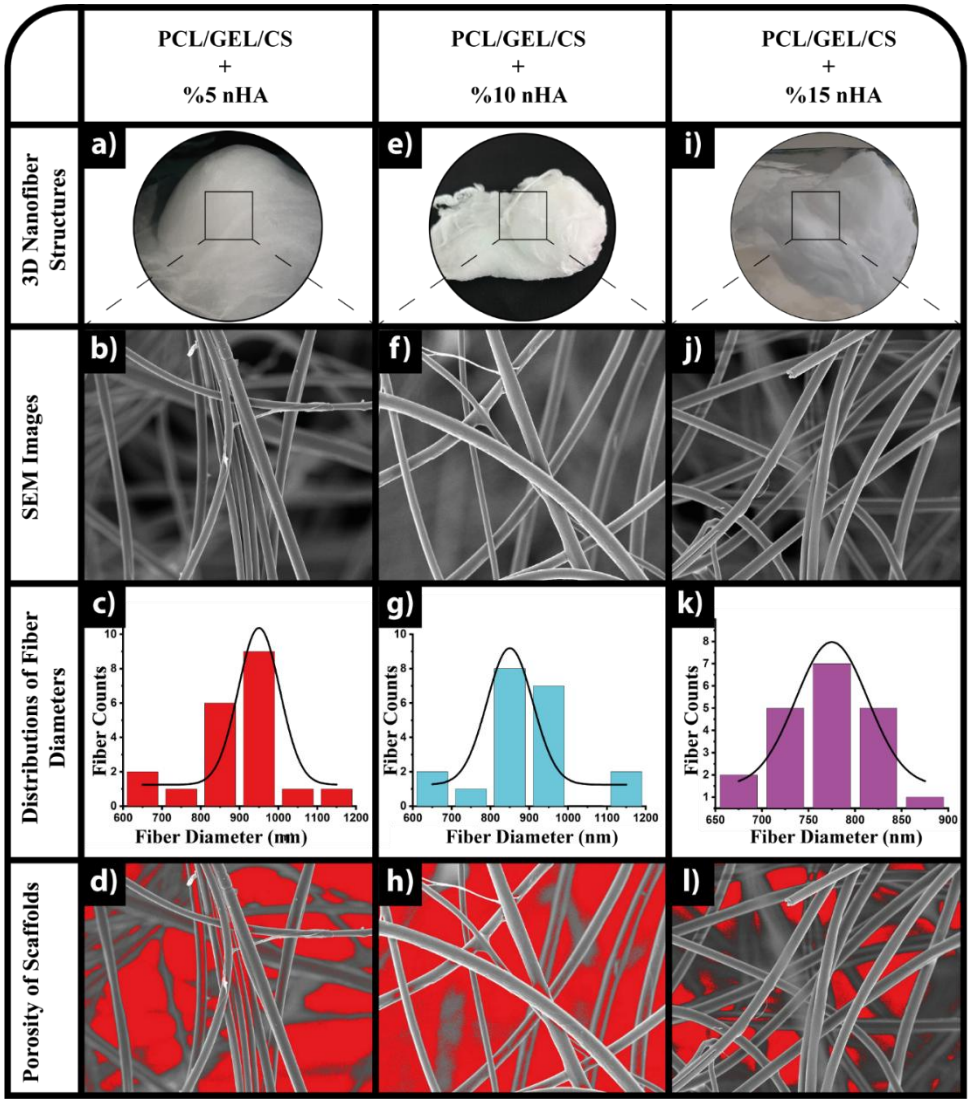


Figure 3. Morphological analysis of PCL/GEL/CS/nHA nanofiber scaffolds containing 5%, 10%, and 15% nHA shows the 3D nanofiber structures, SEM images, fiber diameter distributions, and porosity of the scaffolds for each concentration (respectively).

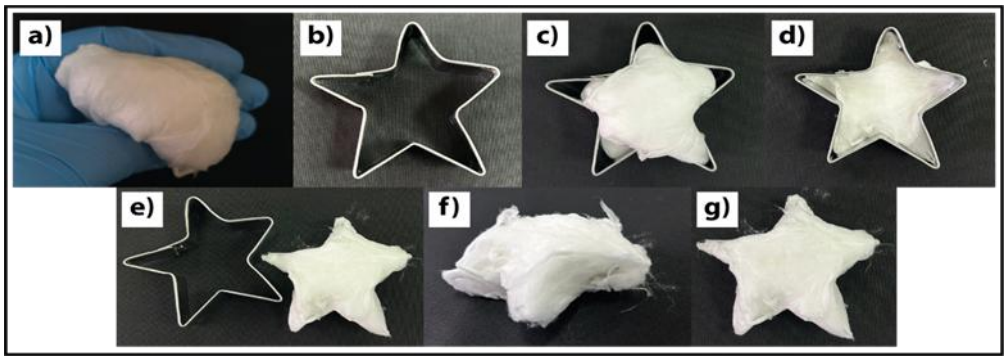


Figure 4. Characteristics of PCL/GEL/nHA nanofiber scaffold structures: a, b, c and d illustrate the scaffold's response to compression, e and f show the scaffold's altered shape from a side perspective, and g displays a lateral view highlighting the scaffold's ability to be molded in three dimensions.

3.3. FTIR Spectroscopy

The FTIR spectra of the PCL-GEL-CS and PCL-GEL-CS-nHA samples reveal the characteristic absorption bands of the respective components (Figure 5). In both samples, PCL shows distinctive C–H stretching vibrations at ~2940 and 2866 cm^{-1}, and a strong carbonyl (C=O) stretching band around 1722 cm^{-1}. The presence of gelatin and chitosan is confirmed by the Amide I band (~1637 cm^{-1}) and the Amide II band (~1533 cm^{-1}). Upon incorporation of nano hydroxyapatite (nHA), a noticeable increase in the intensity of the absorption band near ~1029 cm^{-1} is observed, corresponding to the PO_4^{3-} stretching vibrations. This spectral change confirms the successful integration of nHA into the composite matrix. The overall preservation of PCL and gelatin/chitosan bands alongside the appearance of phosphate-related peaks indicates that the scaffold successfully incorporates both organic and inorganic phases, which is consistent with previous findings reported in the literature [23]–[27].

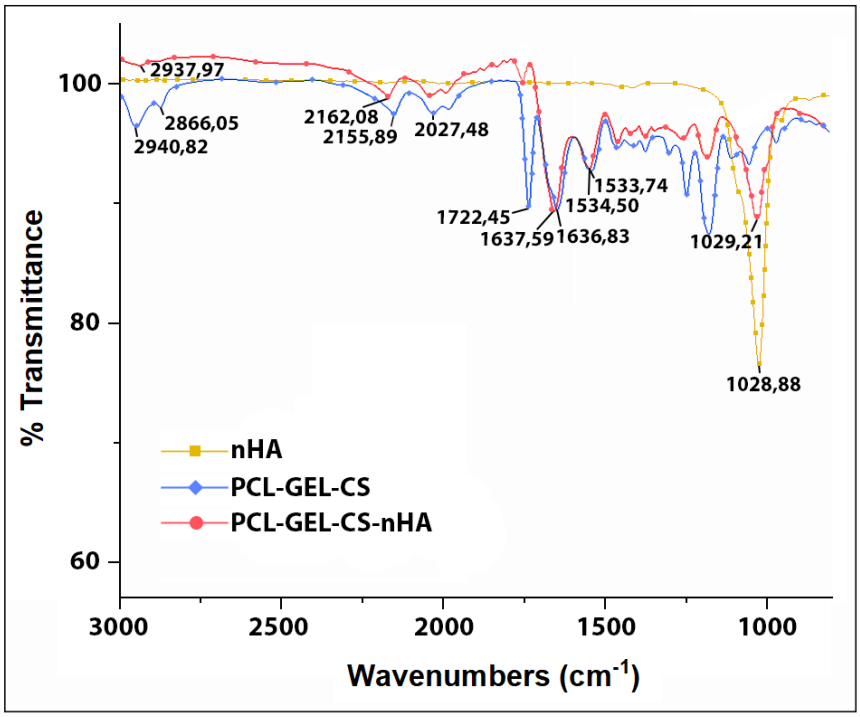


Figure 5. FTIR spectra of nHA, PCL-GEL-CS, and PCL-GEL-CS-nHA samples showing characteristic functional groups and confirming nHA incorporation into the composite structure.

3.4. WVTR, Swelling and Biodegradation Analysis

In scaffolds designed for bone tissue repair, maintaining an appropriate water vapor transmission rate (WVTR) is essential to support cellular viability and integration with the surrounding tissue. A balanced WVTR ensures sufficient gaseous exchange while preventing both scaffold dehydration and excessive fluid accumulation, conditions that could otherwise impair cellular activities [26], [27]. The PCL-GEL-CS-nHA scaffold exhibited a WVTR of approximately 204.35 $mg/m^2 \cdot h$, indicating moderate permeability to water. This level of permeability fosters a moist and breathable microenvironment conducive to osteoblast adhesion and proliferation, closely mimicking the conditions of native tissues [25], [26]. These findings are consistent with results reported in similar applications [28].

Water absorption analysis revealed a swelling ratio of 87.18% on the first day, attributed to the hydrophilic nature of gelatin and chitosan components, and further enhanced by hydroxyapatite surface modification [26]–[29] (Figure 6).

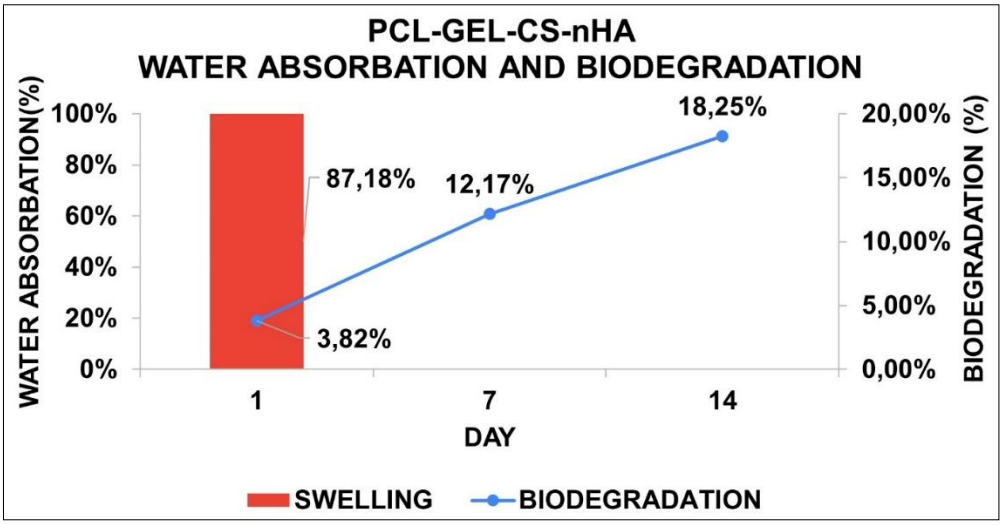


Figure 6. Water absorption and biodegradation profile of PCL-GEL-CS-nHA scaffold over 7 days, highlighting high initial swelling (87.18%) and a gradual increase in biodegradation up to 12.17%.

When evaluated in terms of biodegradability, the scaffold showed a gradual degradation reaching 18.25% within 14 days. This indicates a controlled degradation process suitable for tissue engineering applications. A controlled degradation profile is vital to maintain mechanical integrity in the early stages of tissue regeneration and to allow gradual tissue growth and scaffold resorption over time [24], [25]. The swelling and degradation behaviors are similar to the trends previously observed in PCL/GEL/CS-based systems modified with bioceramics such as HA. Such additives provide a balanced structure between mechanical strength and biodegradability [27], [29].

Overall, the PCL-GEL-CS-HA scaffold demonstrated a combination of high water absorption capacity, controlled water transport, and moderate degradation rate, which are critical to ensure cell viability, proliferation, and eventual replacement of the scaffold by newly formed tissue. These findings are in agreement with previous reports indicating that composite scaffolds containing hydroxyapatite with polymeric matrices exhibit superior physicochemical and biological properties suitable for bone tissue engineering applications [24]–[29].

3.5. Biological Relevance and Expected Performance of PCL/GEL/CS/nHA 3D Scaffolds

Although the present study primarily focuses on the morphological and physicochemical characterization of the newly developed 3D PCL/GEL/CS/nHA scaffolds, their strong potential for bone tissue engineering is well supported by extensive evidence reported in the literature. The complementary properties of PCL, gelatin, chitosan, and nano-hydroxyapatite (nHA) provide an inherently bioactive platform capable of effectively supporting osteogenic processes.

PCL contributes the necessary mechanical stability and structural robustness that make it a widely used polymer in bone tissue engineering applications [30]. Gelatin enhances cellular adhesion and proliferation through its RGD-containing protein-derived functional groups, which facilitate integrin-mediated cell attachment. Chitosan provides additional bioactivity through its osteoconductive and antimicrobial characteristics, both of which have been repeatedly shown to improve cell–material interactions and support bone regeneration. The successful and homogeneous incorporation of nHA confirmed through FTIR plays a critical role, as nHA mimics the mineral phase of natural bone and is widely recognized for promoting osteoblast attachment, proliferation, and differentiation. The expected biological functionality of this composite structure is strongly aligned with previously published findings. Hydroxyapatite-based scaffolds fabricated by DLP 3D printing have been shown to exhibit excellent cytocompatibility, with cell viability exceeding 70% and clear evidence of enhanced osteoblast adhesion and proliferation [31]. Similarly, tri-polymer scaffolds containing gelatin and chitosan have demonstrated marked improvements in cell adhesion, viability, proliferation, and biomineralization due to the synergistic interactions among these natural polymers [32]. These results collectively confirm that the material components used in our scaffold are well established for enhancing osteogenic activity.

Additionally, the unique cotton-like 3D architecture produced using the spherical collector offers up to 79% porosity, enabling efficient nutrient diffusion, waste removal, and deep cellular infiltration conditions essential for vascularization and successful in vivo tissue integration. Based on the established biological behavior of the constituent materials and the structural advantages of the fabricated scaffold, the PCL/GEL/CS/nHA system is expected to support high cell viability, robust osteoblast adhesion, and superior osteogenic differentiation capability.

4. CONCLUSION and SUGGESTIONS

This study demonstrated that cotton-like, highly porous, three-dimensional (3D) nanofiber scaffolds composed of a PCL/GEL/CS/nHA blend could be successfully produced using an optimized single-step electrospinning method employing a specially designed spherical collector. This spherical collector is a partially conductive, semi-spherical structure that enables the omnidirectional deposition of fibers and the formation of 3D structures, in contrast to traditional flat collectors. The spherical collector approach, which constitutes the main novelty of this work, overcomes the limitations of conventional 2D electrospun membranes, allowing for the fabrication of true 3D scaffolds that are compressible, shapeable, and conformable to the geometry of complex bone defects. Morphological analyses showed that increasing nHA content decreased fiber diameters from 950 ± 44 nm to 775 ± 11 nm and reduced porosity from 79% to 70%, resulting in a denser and interconnected network structure.

Physicochemical assessments confirmed that the scaffold offers a balanced water vapor transmission rate (204.35 mg/m^2), a high swelling capacity (87.18%), and a controlled biodegradation profile (18.25% in 14 days). When considered together, these properties indicate that the developed PCL/GEL/CS/nHA scaffolds create a suitable microenvironment that supports osteogenic cell attachment, proliferation, and tissue regeneration. Consequently, these innovative 3D cotton-like scaffolds are a strong candidate for bone tissue engineering; however, in vivo biological evaluations are required in later stages to confirm their clinical efficacy.

Acknowledgment

This research was supported by Muğla Sıtkı Koçman University Scientific Research Projects Coordination Office (Project No: 24/168/02/1)

Conflict of Interest Statement

There is no conflict of interest between the authors.

Statement of Research and Publication Ethics

The study is complied with research and publication ethics

Artificial Intelligence (AI) Contribution Statement

This manuscript was entirely written, edited, analyzed, and prepared without the assistance of any artificial intelligence (AI) tools. All content, including text, data analysis, and figures, was solely generated by the authors.

Contributions of the Authors

Ö.E.: Research, Experimentation, Visualization, Resources, H.Ş.D.: Research, Experimentation, Visualization, Resources, U.E.: Research, Visualization, Writing – original draft, H.S.: Research, Idea Owner, Experiment Design, Writing

REFERENCES

[1] C. Ferguson, E. Alpern, T. Miclau, and J. A. Helms, "Does adult fracture repair recapitulate embryonic skeletal formation?," *Mech. Dev.*, vol. 87, no. 1–2, pp. 57–66, 1999, doi: 10.1016/S0925-4773(99)00142-2.

[2] W. Sieiński, "Endometrial stromal neoplasms of the uterus. A clinicopathologic study.," *Patol. Pol.*, vol. 43, no. 1, pp. 30–34, 1992.

[3] A. H. Schmidt, "Autologous bone graft: Is it still the gold standard?," *Injury*, vol. 52, pp. S18–S22, 2021, doi: 10.1016/j.injury.2021.01.043.

[4] R. Betz and M. D. R., "Limitations of autograft and allograft: New synthetic solutions.," pp. S561–S570, 2002.

[5] V. Campana *et al.*, "Bone substitutes in orthopaedic surgery: from basic science to clinical practice," *J. Mater. Sci. Mater. Med.*, vol. 25, no. 10, pp. 2445–2461, 2014, doi: 10.1007/s10856-014-5240-2.

[6] H. J. Haugen, S. P. Lyngstadaas, F. Rossi, and G. Perale, "Bone grafts: which is the ideal biomaterial?," *J. Clin. Periodontol.*, vol. 46, no. S21, pp. 92–102, 2019, doi: 10.1111/jcpe.13058.

[7] A. Odén, E. V. McCloskey, J. A. Kanis, N. C. Harvey, and H. Johansson, "Burden of high fracture probability worldwide: secular increases 2010–2040," *Osteoporos. Int.*, vol. 26, no. 9, pp. 2243–2248, 2015, doi: 10.1007/s00198-015-3154-6.

[8] G. Battafarano *et al.*, "Strategies for bone regeneration: From graft to tissue engineering," *Int. J. Mol. Sci.*, vol. 22, no. 3, pp. 1–22, 2021, doi: 10.3390/ijms22031128.

[9] A. Grémare *et al.*, "Characterization of printed PLA scaffolds for bone tissue engineering," *J. Biomed. Mater. Res. - Part A*, vol. 106, no. 4, pp. 887–894, 2018, doi: 10.1002/jbm.a.36289.

[10] M. Zienkiewicz-Strzałka, A. Deryło-Marczewska, Y. A. Skorik, V. A. Petrova, A. Choma, and I. Komaniecka, "Silver nanoparticles on chitosan/silica nanofibers: Characterization and antibacterial activity," *Int. J. Mol. Sci.*, vol. 21, no. 1, 2020, doi: 10.3390/ijms21010166.

[11] F. Cestari, M. Petretta, Y. Yang, A. Motta, B. Grigolo, and V. M. Sglavo, "3D printing of PCL/nano-hydroxyapatite scaffolds derived from biogenic sources for bone tissue engineering," *Sustain. Mater. Technol.*, vol. 29, no. July, p. e00318, 2021, doi: 10.1016/j.susmat.2021.e00318.

[12] F. Liu *et al.*, "Preparation and antibacterial properties of ε-polylysine-containing gelatin/chitosan nanofiber films," *Int. J. Biol. Macromol.*, vol. 164, pp. 3376–3387, 2020, doi: 10.1016/j.ijbiomac.2020.08.152.

[13] R. Yao, J. He, G. Meng, B. Jiang, and F. Wu, "Electrospun PCL/Gelatin composite fibrous scaffolds: Mechanical properties and cellular responses," *J. Biomater. Sci. Polym. Ed.*, vol. 27, no. 9, pp. 824–838, 2016, doi: 10.1080/09205063.2016.1160560.

[14] H. Elkhouly, W. Mamdouh, and D. I. El-Korashy, "Electrospun nano-fibrous bilayer scaffold prepared from polycaprolactone/gelatin and bioactive glass for bone tissue engineering," *J. Mater. Sci. Mater. Med.*, vol. 32, no. 9, 2021, doi: 10.1007/s10856-021-06588-6.

[15] V. Brun *et al.*, "Chitosan/hydroxyapatite hybrid scaffold for bone tissue engineering," *Biomed. Mater. Eng.*, vol. 24, no. 1, pp. 63–73, 2014, doi: 10.3233/BME-140975.

[16] H. Zhou and J. Lee, "Nanoscale hydroxyapatite particles for bone tissue engineering," *Acta Biomater.*, vol. 7, no. 7, pp. 2769–2781, 2011, doi: 10.1016/j.actbio.2011.03.019.

[17] L. Lauro *et al.*, "Coated electrospun bioactive wound dressings : Mechanical properties and ability to control lesion microenvironment," *Mater. Sci. Eng. C*, vol. 100, no. October 2018, pp. 493–504, 2019, doi: 10.1016/j.msec.2019.03.005.

[18] A. A. M. Shimojo, A. G. M. Perez, S. E. M. Galdames, I. C. S. Brissac, and M. H. A. Santana, "Stabilization of porous chitosan improves the performance of its association with platelet-rich plasma as a composite scaffold," *Mater. Sci. Eng. C*, vol. 60, pp. 538–546, 2016, doi: 10.1016/j.msec.2015.11.080.

[19] F. Mohammad, B. Kaffashi, and P. Shokrollahi, "PCL / chitosan / Zn-doped nHA electrospun nanocomposite scaffold promotes adipose derived stem cells adhesion and proliferation," *Carbohydr. Polym.*, vol. 118, pp. 133–142, 2015, doi: 10.1016/j.carbpol.2014.10.071.

[20] M. Yılmaz and A. Altan, "Elektroeğirme Yöntemine Dayalı Nanosensörlerin Gıda Alanındaki Uygulamalari," *Gida / J. Food*, vol. 42, no. 6, pp. 708–725, 2017, doi: 10.15237/gida.gd17057.

[21] H. Zhong, J. Huang, J. Wu, and J. Du, "Electrospinning nanofibers to 1D , 2D , and 3D scaffolds and their biomedical applications," vol. 15, no. 2, pp. 787–804, 2022.

[22] S. Dai, H. Liang, M. Zhu, and Y. Zhang, "Electrospun silk for biomedical applications," *Med-X*, 2024, doi: 10.1007/s44258-024-00038-y.

[23] I. M. Sek, "Fabrication of Two- and Three- Dimensional Fibrous Mats by Electrospinning Method," vol. I, no. 1, pp. 31–38, 2018.

[24] S. Gautam *et al.*, "Gelatin-polycaprolactone-nanohydroxyapatite electrospun nanocomposite scaffold for bone tissue engineering," *Mater. Sci. Eng. C*, vol. 119, no. September 2020, p. 111588, 2021, doi: 10.1016/j.msec.2020.111588.

[25] Z. Ebrahimi, S. Irani, A. Ardeshirylajimi, and E. Seyedjafari, "Enhanced osteogenic differentiation of stem cells by 3D printed PCL scaffolds coated with collagen and hydroxyapatite," *Sci. Rep.*, pp. 1–15, 2022, doi: 10.1038/s41598-022-15602-y.

[26] S. Gautam *et al.*, "Surface modification of PCL-gelatin-chitosan electrospun scaffold by nano-hydroxyapatite for bone tissue engineering," *Mater. Today Commun.*, vol. 34, no. August 2022, p. 105237, 2023, doi: 10.1016/j.mtcomm.2022.105237.

[27] J. Liu *et al.*, "Polycaprolactone/Gelatin/Hydroxyapatite Electrospun Nanomembrane Materials Incorporated with Different Proportions of Attapulgite Synergistically Promote Bone Formation," *Int. J. Nanomedicine*, vol. 17, no. August, pp. 4087–4103, 2022, doi: 10.2147/IJN.S372247.

[28] M. Zhang, X. Qiao, W. Han, T. Jiang, F. Liu, and X. Zhao, "Alginate-chitosan oligosaccharide-ZnO composite hydrogel for accelerating wound healing," *Carbohydr. Polym.*, vol. 266, no. February, p. 118100, 2021, doi: 10.1016/j.carbpol.2021.118100.

[29] R. M. Jin, N. Sultana, S. Baba, S. Hamdan, and A. F. Ismail, "Porous PCL/Chitosan and nHA/PCL/chitosan scaffolds for tissue engineering applications: Fabrication and evaluation," *J. Nanomater.*, vol. 2015, 2015, doi: 10.1155/2015/357372.

[30] M. A. Woodruff and D. W. Hutmacher, "Progress in Polymer Science The return of a forgotten polymer Polycaprolactone in the 21st century," vol. 35, pp. 1217–1256, 2010, doi: 10.1016/j.progpolymsci.2010.04.002.

[31] R. Das *et al.*, "DLP 3D-printed hydroxyapatite-bioglass composite scaffolds for bone tissue engineering : Structural , mechanical , biological , and antibacterial evaluations," *Mater. Today Chem.*, vol. 48, no. July, p. 102925, 2025, doi: 10.1016/j.mtchem.2025.102925.

[32] A. Kumar, S. Krishna, and A. Biswas, "Constructing a biofunctionalized 3D-printed gelatin / sodium alginate / chitosan tri-polymer complex scaffold with improvised biological and mechanical properties for bone-tissue engineering," *Bio-Design Manuf.*, vol. 7, no. 1, pp. 57–73, 2024, doi: 10.1007/s42242-023-00249-z.